THE JOURNAL OF BIOLOGICAL CHEMISTRY VOL. 289, NO. 37, pp. 25879–25889, September 12, 2014
© 2014 by The American Society for Biochemistry and Molecular Biology, Inc. Published in the U.S.A.

Progranulin Transcripts with Short and Long 5′ Untranslated Regions (UTRs) Are Differentially Expressed via Posttranscriptional and Translational Repression*

Received for publication, February 21, 2014, and in revised form, July 22, 2014 Published, JBC Papers in Press, July 23, 2014, DOI 10.1074/jbc.M114.560128

Anja Capell[‡1], **Katrin Fellerer**[‡], **and Christian Haass**[‡§¶2]

From the [‡]*Adolf-Butenandt Institute, Biochemistry, Ludwig-Maximilians University Munich, 80336 Munich, Germany, the* [§]*German Center for Neurodegenerative Diseases (DZNE), 80336 Munich, Germany, and the* [¶]*Munich Cluster for Systems Neurology (SyNergy), 80336 Munich, Germany*

Background: Haploinsufficiency of progranulin is a major cause of familial frontotemporal lobar degeneration.
Results: Expression of progranulin is differentially repressed by a unique 5′ untranslated region.
Conclusion: Expression of progranulin is tightly controlled at the translational and transcriptional level.
Significance: Understanding the physiological regulation of progranulin expression may allow the development of therapeutic approaches to restore reduced levels of progranulin in patients.

Frontotemporal lobar degeneration is associated with cytoplasmic or nuclear deposition of the TAR DNA-binding protein 43 (TDP-43). Haploinsufficiency of progranulin (GRN) is a major genetic risk factor for frontotemporal lobar degeneration associated with TDP-43 deposition. Therefore, understanding the mechanisms that control cellular expression of GRN is required not only to understand disease etiology but also for the development of potential therapeutic strategies. We identified different GRN transcripts with short (38–93 nucleotides) or long (219 nucleotides) 5′ UTRs and demonstrate a cellular mechanism that represses translation of GRN mRNAs with long 5′ UTRs. The long 5′ UTR of GRN mRNA contains an upstream open reading frame (uORF) that is absent in all shorter transcripts. Because such UTRs can be involved in translational control as well as in mRNA stability, we compared the expression of GRN in cells expressing cDNAs with and without 5′ UTRs. This revealed a selective repression of GRN translation and a reduction of mRNA levels by the 219-nucleotide-long 5′ UTR. The specific ability of this GRN 5′ UTR to repress protein expression was further confirmed by its transfer to an independent reporter. Deletion analysis identified a short stretch between nucleotides 76 and 125 containing two start codons within one uORF that is required and sufficient for repression of protein expression. Mutagenesis of the two AUG codons within the uORF is sufficient to reduce translational repression. Therefore initiating ribosomes at the AUGs of the uORF fail to efficiently initiate translation at the start codon of GRN. In parallel the 5′ UTR also affects mRNA stability; thus two independent mechanisms determine GRN expression via mRNA stability and translational efficiency.

This is an open access article under the CC BY license.

* This work was supported by the European Research Council under the European Union Seventh Framework Program (FP7/2007-2013)/ERC Grant Agreement No. 321366-Amyloid (advanced grant to C. H.).

[1] To whom correspondence may be addressed: German Center for Neurodegenerative Diseases and Adolf Butenandt Institute, Biochemistry, Ludwig Maximilian University, Schillerstr. 44, 80336 Munich, Germany. Tel.: 49-89-2180-75484; Fax: 49-89-2180-75415; E-mail: anja.capell@mail03.med.uni-muenchen.de.

[2] To whom correspondence may be addressed: German Center for Neurodegenerative Diseases and Adolf Butenandt Institute, Biochemistry, Ludwig Maximilian University, Schillerstr. 44, 80336 Munich, Germany. Tel.: 49-89-2180-75472; Fax: 49-89-2180-75415; E-mail: christian.haass@mail03.med.uni-muenchen.de.

Neurodegenerative diseases such as Alzheimer disease, Parkinson disease, and frontotemporal lobar degeneration (FTLD)[3] are a major threat to our aging society. Among them, FTLD is the second most common cause of dementia in patients under the age of 65 (1, 2). FTLD is a disease spectrum known to show a major clinical and pathological overlap with amyotrophic lateral sclerosis (ALS) (3). Pathologically different subtypes of FTLD are defined by the deposition of disease-characterizing proteins (3). About 40% of FTLD patients develop tau-positive inclusions (FTLD-tau) (3). The remaining patients are characterized by tau-negative, ubiquitin-positive nuclear or cytoplasmic aggregates. TDP-43 is the most frequently deposited protein in tau-negative FTLD cases (FTLD-TDP) (4). TDP-43 is a nucleic acid binding protein that normally localizes to the nucleus. During the disease, TDP-43 is frequently deposited within the cytosol, accompanied by its nuclear clearance (4). The risk for FTLD-TDP is increased dramatically in patients with a haploinsufficiency for progranulin (GRN) (5, 6). Genetic linkage analysis and exome sequencing identified a large number of non-sense mutations that all lead to GRN haploinsufficiency (7). In addition, missense mutations were also found (8–10), which can lead to cytoplasmic missorting of GRN because of a dysfunctional signal peptide or to misfolding and, consequently, to a reduction of GRN secretion (7, 11, 12). Therefore, all FTLD-TDP-associated GRN mutations result in reduced GRN levels. Homozygous mutations in the GRN gene that cause a complete absence of GRN cause neuronal ceroid lipofuscinosis, suggesting that lysosomal dysfunction may also underlie, to some extent, FTLD pathology in patients with GRN haploinsufficiency (13). Interestingly, compounds that inter-

[3] The abbreviations used are: FTLD, frontotemporal lobar degeneration; ALS, amyotrophic lateral sclerosis; GRN, progranulin; EGFP, enhanced GFP; FRT, Flp recombinase target; ANOVA, analysis of variance; TDP, TAR DNA-binding protein.

fere with lysosomal acidification and autophagy, such as bafilomycin A1 or chloroquine, lead to a strong increase in GRN levels and may rescue GRN haploinsufficiency (14). GRN expression is increased not only during lysosomal stress but also in several other pathological conditions such as inflammation, wound healing, tumor genesis, and type 2 diabetes (7). The cellular mechanisms that allow the rapid and robust increase of GRN levels are poorly understood. However, upon interference with lysosomal function, posttranscriptional mechanisms appear to be involved (see, for example, Ref. 14).

Here we identified GRN transcripts with short (38–93 nucleotides) and long (219 nucleotides) 5′ UTRs. We have shown previously that translation of the β-amyloid precursor protein-processing enzymes β-secretase (β-site amyloid precursor protein-cleaving enzyme 1 (BACE1)) and a disintegrin and metalloprotease 10 (ADAM10)) mRNAs are both repressed by their long 5′ UTRs (15, 16). Encouraged by these findings, we investigated whether GRN 5′ UTRs of different lengths may differentially affect GRN translation and levels of GRN mRNA. We provide evidence that the 5′ UTR of GRN contributes to translational repression and mRNA stability.

EXPERIMENTAL PROCEDURES

cDNA Constructs—The human GRN ORF and the 5′ UTR and 3′ UTR were amplified by PCR from HEK 293T cell cDNA and subcloned into the BamHI and EcoRV restriction sites of the inducible pcDNA5/FRT/$TO_{(Hygro)}$ expression vector for the Flp-In™ System (Life Technologies, Invitrogen, Darmstadt, Germany). GRN cDNA constructs were generated either by triple PCR or by site-directed mutagenesis (Stratagene, La Jolla, CA). All GRN cDNA constructs contained the endogenous Kozak consensus sequence (CAGACC) (17) in front of the start codon and a myc tag at the 3′ end of the ORF containing a stop codon. The GRN 5′ UTR with or without a GRN signal peptide was cloned in front of EGFP by triple PCR, and the final PCR product was subcloned into the BamHI and EcoRV restriction sites of the pcDNA5/FRT/$TO_{(Hygro)}$ expression vector. Note that, in addition to the indicated 5′ UTR, the transcripts of all cDNA constructs harbor at their 5′ end 100 vector-derived nucleotides from the region between the putative transcriptional start and the BamHI cloning site. All cDNA constructs were verified by DNA sequencing.

Quantifying mRNA with Real-time Quantitative PCR—For quantitative RT-PCR, total RNA preparation and reverse transcription were performed as described before (14). Quantitative RT-PCRs were carried out on a 7500 Fast real-time PCR system (Applied Biosystems, Carlsbad, CA) with TaqMan technology using human GRN (Hs00963703, exon boundary 3–4), and human GAPDH (4326317E) primer sets (Applied Biosystems). For each cDNA construct, at least three independent samples were analyzed. Reverse-transcribed GRN cDNA was normalized to endogenous GAPDH and expressed as a ratio to the 5′3′ UTR cDNA construct (see Fig. 2 A) levels using the $2^{-\Delta\Delta Ct}$ method.

In Vitro Transcription and Translation—The indicated cDNA constructs in pcDNA4 MycHis with a stop codon before the His tag were linearized, purified by agarose gel electrophoresis, eluted with diethylpyrocarbonate-treated H_2O, and cDNA concentration was adjusted to 0.5 μg/μl. Capped mRNAs were generated using the mMessage mMachine kit (Life Technologies, Ambion, Darmstadt, Germany). After template digestion with DNaseI, the mRNAs were purified with the RNeasy kit (Qiagen, Hilden, Germany), and RNA concentration was adjusted to 0.5 μg/μl. The size and integrity of the mRNAs were assessed by gel electrophoresis. *In vitro* translation reactions were performed in nuclease-treated rabbit reticulocyte lysate as described by the manufacturer (Promega, Madison, WI).

Cell Culture, Stable Cell Lines, and Transient Transfection—The Flp-In™ T-REx™ 293 cell line is a HEK 293 cell line containing a single integrated Flp recombination target (FRT) site. For stable, tetracycline-inducible, isogenic expression, each construct cloned in pcDNA5/FRT/$TO_{(Hygro)}$ was cotransfected with 9/10 cDNA of a Flp recombinase expression plasmid (pOG44, all from Invitrogen). Pooled stable cell lines were selected and cultured with 150 μg/ml hygromycin in DMEM with Glutamax I (Invitrogen), supplemented with 10% (v/v) fetal calf serum (Invitrogen) and penicillin/streptomycin (PAA Laboratories, Pasching, Austria). For plateaued expression levels, cell lines were treated with 0.2 μg/ml tetracycline (Sigma-Aldrich, Munich, Germany) for 24 h before the start of the experiment. Transient transfection of HEK293T cells was carried out using Lipofectamine™ 2000 (Invitrogen).

Antibodies—The following antibodies were used: rabbit polyclonal antibody to human GRN (Invitrogen, 1:700), mouse monoclonal antibody to β-actin, (Sigma-Aldrich, 1:2000), mouse monoclonal antibody to green fluorescent protein (Clontech, Mountain View, CA, 1:2000), and mouse monoclonal antibody (9E10) to c-myc (developed by J. M. Bishop, distributed by the Developmental Studies Hybridoma Bank, NICHD, National Institutes of Health, Department of Biology, University of Iowa, 1:1000). HRP-conjugated goat anti-mouse or goat anti-rabbit IgG (Promega, 1:10,000) was used as a secondary antibody.

Preparation of Conditioned Media, Cell Lysates, and Immunoblotting—Conditioned media and cell lysates were prepared and analyzed as described previously (14). Briefly, conditioned media were centrifuged at 15,000 × *g* for 15 min at 4 °C and either subjected directly to standard 10% SDS-PAGE or to GRN ELISA. After washing with PBS, cells were lysed in ice-cold STEN lysis buffer (150 mM NaCl, 50 mM Tris-HCl (pH 7.6), 2 mM EDTA, and 2% Nonidet P-40, supplemented with protease inhibitor mixture (Sigma-Aldrich)) and clarified by centrifugation. Equal amounts of protein were separated by SDS-PAGE and transferred onto polyvinylidene difluoride membranes. For detection, the indicated antibodies were used. Bound antibodies were visualized by horseradish peroxidase-conjugated secondary antibody using an enhanced chemiluminescence technique (GE Healthcare). Signals for quantification were detected by a luminescent image analyzer (LAS-4000, Fujifilm Life Science, Tokyo, Japan) and evaluated with Multi GaugeV3.0 software.

ELISA for Human GRN—Secreted GRN in conditioned medium was quantified by sandwich ELISA using streptavidin-coated 96-well multiarray plates and the Meso Scale Discovery Sector Imager 2400 for the readout, as described previously (14).

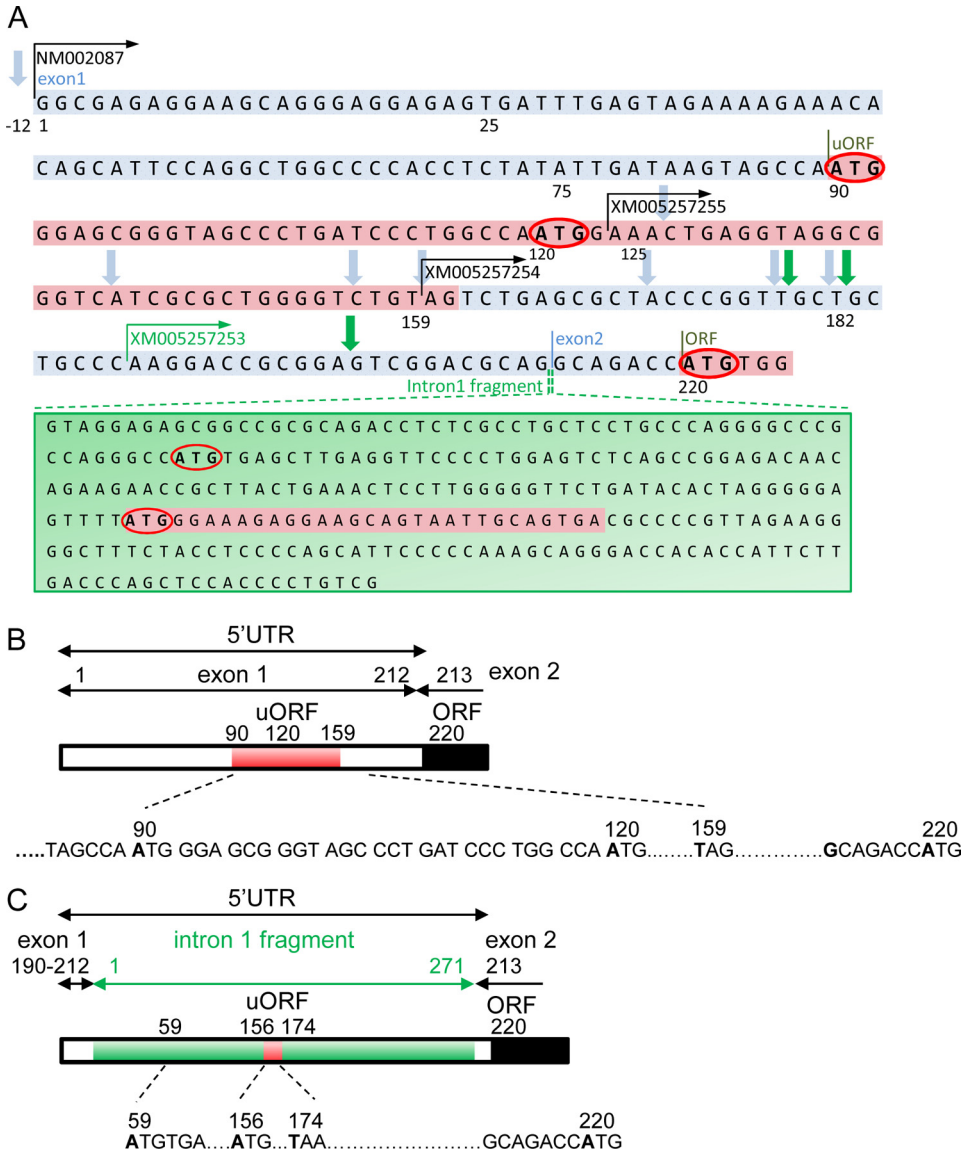

FIGURE 1. **Annotated variants of the GRN 5′ UTR.** *A*, sequence of the 219 nucleotides of the GRN 5′ UTR derived from human brain cDNA. This annotated variant (*NM002087*) and start sites of predicted shorter variants (*XM005257255* and *XM005257254*) are indicated, as well as a predicted splice variant (*XM005257253*) containing a short sequence stretch of exon 1, followed by an insertion of 271 nucleotides of intron 1 (*green box*) at the exon 1/2 boundary. 5′ ends identified by rapid amplification of cDNA ends are marked by *arrows*. *Green arrows* indicate mRNAs containing the intron 1-derived sequence stretch. ORFs are highlighted in *red*, and AUG start codons are *circled*. *B*, schematic of the 219-nucleotide-long GRN 5′ UTR. Two AUG initiation codons (positions 90 and 120), the corresponding uORF, and the stop codon (nucleotides 159–161) are indicated. *C*, schematic of the alternative spliced GRN 5′ UTR (*XM005257253*). This splice variant contains a short stretch of exon 1 (nucleotides 190–212), followed by 271 nucleotides derived from intron 1 containing two AUGs (*circled*) and one short uORF (*156–176*).

Statistics—Statistical analysis was performed using GraphPad Prism 6 (GraphPad Software, San Diego, CA). For comparison of two groups, unpaired Student's *t* test was used with a significance level of 0.05. For multiple comparisons, one-way analysis of variance (ANOVA) was used to determine significance, followed by Tukey's post hoc test.

RESULTS

Identification of GRN 5′ UTRs—We first searched for potential 5′ UTRs by rapid amplification of cDNA ends in HEK 293 cells and could demonstrate the presence of a 219-nucleotide-long 5′ UTR (data not shown) as annotated (*NM 002087*) (Fig. 1, *A* and *B*). Furthermore, the 219-nucleotide-long 5′ UTR could be amplified by PCR from an adult human brain cDNA (OriGene Technologies, Rockville, MD) (data not shown). In addition, we identified several shorter 5′ UTRs by 5′ rapid amplification of cDNA ends that were in line with previous computational predictions (*XM005257254/XM005257255*) (Fig. 1*A*). We also found a so far undescribed alternative splice variant of GRN mRNA. This variant skips the exon1/intron1 splice site and includes 271 nucleotides of the intron 1 (*XM005257253*) (Fig. 1, *A* and *C*).

Repression of GRN Expression by Its 5′ UTR—In contrast to the short transcripts, the 219-nucleotide GRN 5′ UTR (*i.e.* long 5′ UTR) contains two AUG start codons (Fig. 1, *A* and *B*), which are within a single short uORF. Such short uORFs are frequently found in transcripts that are regulated via translational mechanisms (18–22). Therefore, we investigated whether the

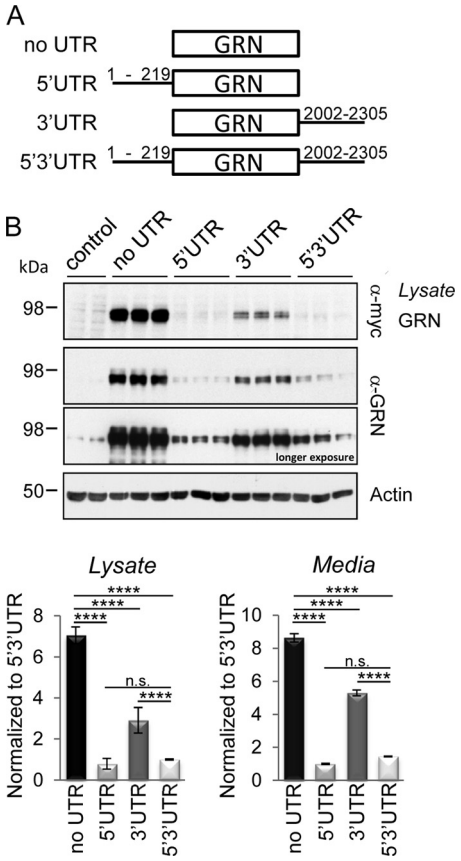

FIGURE 2. **GRN expression is inhibited by its 5′-UTR.** *A*, cDNA constructs used to evaluate the effects of the 5′ and the 3′ UTR on GRN expression. *B*, isogenic expression of the cDNA constructs shown in *A* in HEK 293 cells. GRN expression was investigated in cell lysates by Western blotting using an anti-myc or anti-GRN antibody. Actin was used as loading control. Quantitation of the expression levels of GRN in cell lysates and of secreted GRN is shown in the *bottom panel*. Levels are normalized to the expression of the 5′-3′ UTR. Secreted GRN was analyzed using an ELISA assay described previously (14). For all quantifications, data are mean ± S.D. ($n \geq 3$ independent experiments). ****, $p < 0.0001$, *n.s.*, not significant. ANOVA followed by Tukey's multiple comparison test was used to determine significance.

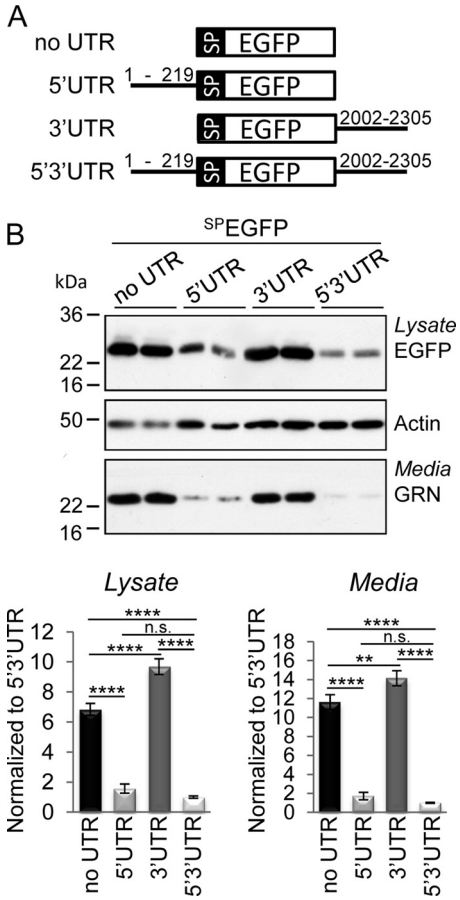

FIGURE 3. **The GRN 5′ UTR inhibits expression of an EGFP reporter.** *A*, schematic showing cDNA constructs used to evaluate the effects of the 5′ UTR, 3′ UTR, and both 5′3′ UTR of GRN on EGFP expression. To allow secretion of EGFP, the coding sequence of EGFP was fused to the signal peptide (*SP*) derived from GRN (*SPEGFP*). *B*, isogenic expression of SPEGFP variants with and without the GRN 5′ UTR, 3′ UTR, and 5′3′ UTR. Actin was used as a loading control. *Bottom panel*, expression levels of SPEGFP in cell lysates and corresponding media were quantified. All quantifications were normalized to 5′3′ UTR constructs. Data are mean ± S.D. ($n \geq 3$ independent experiments). **, $p < 0.01$; ****, $p < 0.0001$; *n.s.*, not significant. ANOVA followed by Tukey's multiple comparison test was used to determine significance.

219-nucleotide GRN 5′ UTR may affect expression of the GRN protein. To do so, we generated GRN variants with and without the 219-nucleotide 5′ UTR (Fig. 2*A*). We also added the GRN 3′ UTR to the 5′ UTR variants to investigate any possibility of additional effects (Fig. 2*A*). To achieve isogenic expression, we used stably transfected Flp-In™ T-REx™ HEK 293 cells in this and all other experimental setups. Strikingly, GRN lacking its 5′ UTR showed a strongly increased expression in cell lysates as well as in conditioned media compared with the GRN variants containing the 5′ UTR or the 5′ and 3′ UTR (Fig. 2*B*). Therefore, these results demonstrate that GRN protein expression is repressed by the 219-nucleotides long 5′ UTR. Although GRN containing only the 3′ UTR showed increased expression compared with GRN with the 5′ UTR or the 5′ and 3′ UTR, the expression was still significantly lower than GRN lacking both UTRs (Fig. 2*B*). This suggests that the 3′ UTR may also contribute to repression of GRN expression. However, the addition of the 3′ UTR to 5′ UTR GRN (5′3′ UTR GRN) did not further lower GRN expression levels (Fig. 2*B*).

To provide further evidence that the 5′ UTR of GRN is directly involved in reducing GRN expression, we fused the GRN 5′ UTR to an EGFP reporter (Fig. 3*A*). Because GRN is a secreted protein, we added the GRN signal peptide to EGFP, allowing its translocation into the endoplasmic reticulum and, consequently, its secretion (Fig. 3*A*). In line with the results shown above, the 5′ UTR significantly repressed expression of EGFP in cell lysates (Fig. 3*B*). Furthermore, production of secreted EGFP was also strongly repressed by the GRN 5′ UTR sequence (Fig. 3*B*), whereas the GRN 3′ UTR had no effect on EGFP expression (Fig. 3*B*). Therefore, the 5′ UTR exhibits an intrinsic repressor function for GRN expression that is independent of the downstream coding sequence.

The GRN 5′ UTR Interferes with GRN Translation and mRNA Stability—With the experiments described above, we could not distinguish the effects of the UTRs on mRNA levels or protein translation. To prove that the 5′ and 3′ UTR of GRN interferes with protein translation, we performed an *in vitro* translation assay using equal amounts of *in vitro* transcribed GRN mRNA (Fig. 4*A*). Upon *in vitro* translation of GRN mRNA lacking the 5′ UTR, robust amounts of protein were obtained, whereas mRNAs containing the 5′ UTR were much less effi-

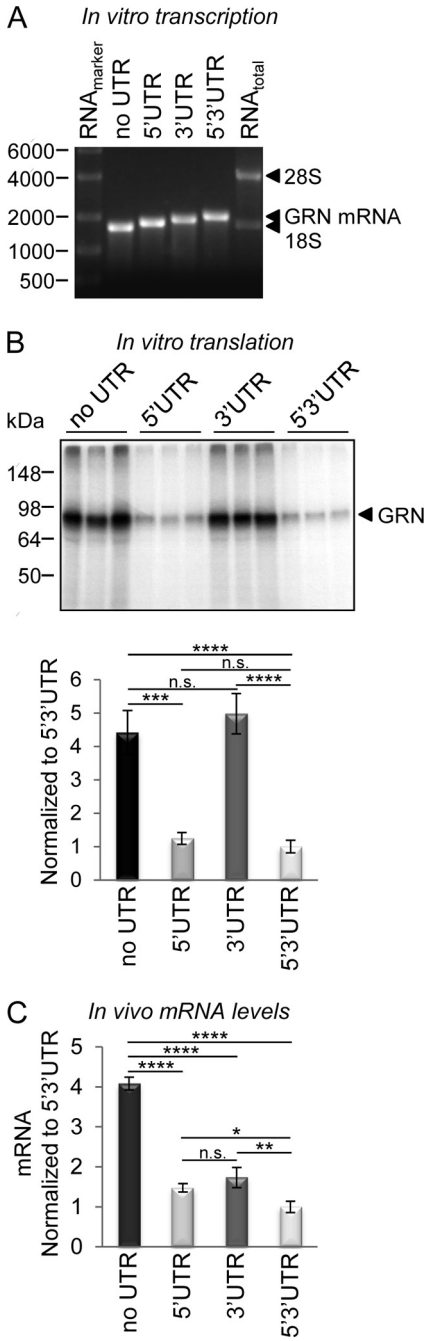

FIGURE 4. **Inhibition of GRN expression occurs at the translational and mRNA levels.** *A*, mRNAs encoding the indicated GRN variants were transcribed *in vitro*. *B*, equal amounts of *in vitro* transcribed mRNAs (~1 μg, adjusted to the number of nucleotides per individual mRNA) were used for in *vitro* translation. Note that the 3′ UTR does not affect GRN translation, whereas the 5′ UTR strongly represses GRN translation. *Bottom panel*, quantitation of the expression levels of GRN upon *in vitro* translation of equal amounts of mRNA normalized to expression of the 5′3′ UTR cDNA construct. *C*, quantitation of GRN mRNA in stable cell lines expressing the indicated cDNA constructs. Levels are normalized to expression of the 5′3′ UTR cDNA construct. Data are mean ± S.D. ($n \geq 3$ independent experiments). *, $p < 0.05$; **, $p < 0.01$; ***, $p < 0.001$; ****, $p < 0.0001$; *n.s.*, not significant. Note that the 5′ and 3′ UTR contributes to a destabilization of GRN mRNA in cells. ANOVA followed by Tukey's multiple comparison test was used to determine significance.

ciently translated (Fig. 4*B*). In contrast, the presence of the 3′ UTR did not repress GRN translation (Fig. 4*B*), supporting the conclusion that only the 5′ UTR, but not the 3′ UTR, selectively

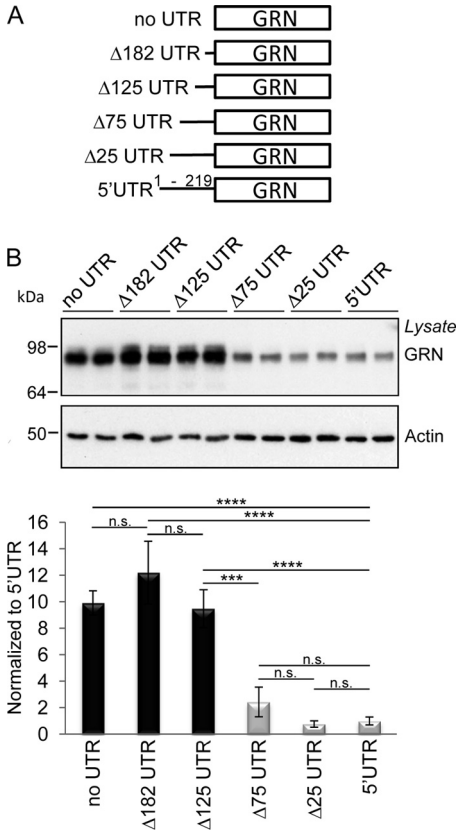

FIGURE 5. **Identification of a 50-nucleotide sequence that is sufficient to repress GRN expression.** *A*, schematic of the sequential deletions constructed to identify the sequence responsible for translational inhibition within the 5′ UTR. *B*, isogenic expression of the deletion constructs shown in *A* reveals a sequence between nucleotides 75 and 125 to be sufficient for translational repression of GRN. *Bottom panel*, quantitation of the expression levels of various deletion constructs normalized to the 5′ UTR construct. Data are mean ± S.D. ($n \geq 3$ independent experiments). ***, $p < 0.001$; ****, $p < 0.0001$; *n.s.*, not significant. Significance was determined by one-way ANOVA followed by Tukey's multiple comparison test.

represses GRN translation. Because the presence of the GRN 3′ UTR resulted in reduced GRN expression levels (see Fig. 2*B*), we investigated whether reduced mRNA levels of the stably transfected isogenic HEK cell line were responsible for the low GRN expression of the 3′ UTR construct. Analysis of mRNA revealed significantly reduced levels not only for the variant, which contains the 3′ UTR, but also for the variant 5′ UTR (Fig. 4*C*). Therefore, both UTRs reduce GRN mRNA, most likely via mRNA destabilization. Differences in transcription were not expected because we used an isogenic system. Therefore, the 5′ UTR represses GRN production via translational inhibition and mRNA reduction.

A 50-Nucleotide Stretch of the UTR Is Required for Repression of GRN Expression—To directly determine which sequence stretch within the 5′ UTR is responsible for the inhibition of GRN expression, we generated a variety of serial deletion constructs (Fig. 5*A*). The deletions included one cDNA construct that lacked nucleotides 1–125 of the 5′ UTR (Δ125 UTR). This construct, which is similar to the shorter transcript described in Fig. 1*A* (XM005257255), lacks both AUG codons present in the long variant. Expression analysis revealed that the first 75 nucleotides of the 5′ UTR of GRN could be removed without significant consequences for translational inhibition (Fig. 5*B*). Interestingly, removing an additional 50 nucleotides (Fig. 5*A*,

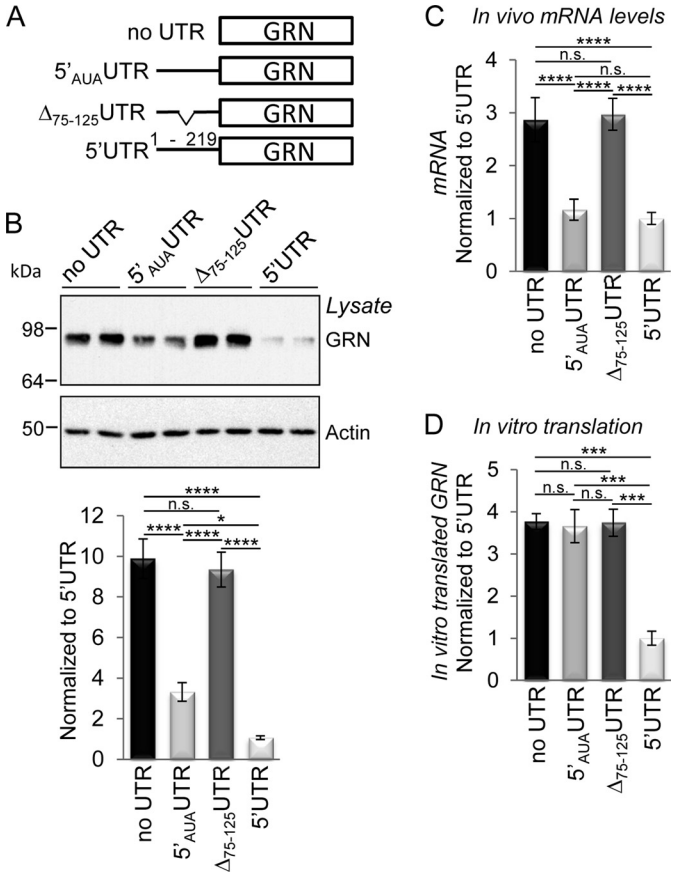

FIGURE 6. **A 50-nucleotide stretch within the 5′ UTR of GRN is required for translational inhibition and lowering of mRNA levels.** *A*, schematic of investigated cDNA constructs. *B*, deletion of nucleotides 75–125 (Δ*75–125*) is sufficient to abolish repression of GRN expression, whereas mutagenesis of both in-frame AUGs within the 5′ UTR increases GRN expression to a significantly lower extent. *Bottom panel*, quantitation of the expression levels of the GRN variants shown in the *top panel*. Expression is normalized to the 5′ UTR cDNA construct. Data are mean ± S.D. ($n \geq 3$ independent experiments). *, $p < 0.05$; ****, $p < 0.0001$; *n.s.*, not significant. *C*, quantitation of GRN mRNA in cell lines expressing the indicated cDNA constructs. Levels are normalized to expression of the 5′ UTR cDNA construct. Data are mean ± S.D. ($n \geq 3$ independent experiments). ****, $p < 0.0001$; *n.s.*, not significant. Note that deletion of nucleotides 75–125 (Δ*75–125*) is sufficient to block the reduction of mRNA levels, whereas mutation of the two AUGs within the 5′ UTR fails to stabilize mRNA levels. *D*, equal amounts of mRNAs transcribed *in vitro* encoding the indicated GRN variants were translated *in vitro*. For quantitation, levels of *in vitro* translated GRN protein were normalized to the 5′ UTR variant. Deletion of nucleotides 75–125 (Δ*75–125*) as well as mutagenesis of the two AUGs within the 5′ UTR leads to a complete loss of translational inhibition. Data are mean ± S.D. ($n \geq 3$ independent experiments). ***, $p < 0.001$; *n.s.*, not significant. Significance was determined by one-way ANOVA followed by Tukey's multiple comparison test.

Δ*125 UTR*) resulted in significantly increased expression and completely abolished repression of GRN expression similar to the constructs missing the entire 5′ UTR (Fig. 5*B*, *no UTR*) or containing only a very short 5′ UTR (Fig. 5*B*, Δ*182*). Therefore, all identified GRN transcripts with shorter 5′ UTRs that lacked the first 125 nucleotides (Δ125 UTR), including the annotated variants XM005257255 and XM005257254, failed to repress GRN expression in contrast to the GRN transcript with the 219-nucleotide 5′ UTR. This also suggests that a short sequence stretch of 50 nucleotides might be required for inhibition of GRN expression. To confirm that this sequence is indeed required for repression of GRN expression, we deleted nucleotides 75–125 (Fig. 6*A*, Δ*75–125*). In line with the data shown above, this short sequence stretch is indispensable for repression of GRN expression by the 5′ UTR of GRN (Fig. 6*B*). Because the stretch between nucleotides 75–125 contains the two AUG start codons described above, we mutated both separately (data not shown) and in combination (Fig. 6*A*, *5′$_{AUA}$-UTR*). Although the mutation of a single start codon had no effect on expression (data not shown), the mutation of both AUGs resulted in a slight but significant increase of GRN expression compared with the long 5′ UTR of GRN (Fig. 6*B*).

The incomplete rescue of GRN expression upon mutagenesis of the two start codons implicates overlaying effects on translation and mRNA levels. To distinguish between these two options, we first analyzed mRNA levels. Indeed, the mRNA level of the 5′$_{AUA}$ UTR variant was similar to that of the 5′ UTR variant and 3-fold lower than for GRN containing no UTR or the deletion variant Δ_{75-125}-UTR (Fig. 6*C*). Therefore, reduced mRNA levels might be responsible for the impaired rescue of expression of the 5′$_{AUA}$-UTR variant. To prove that the mutagenesis of the two AUGs is capable of increasing protein translation, we performed an *in vitro* translation assay using equal amounts of *in vitro* transcribed GRN mRNA. Although the 5′ UTR severely abolished *in vitro* translation of GRN, mutagenesis of the two AUGs was sufficient to obtain GRN levels similar to those translated from GRN mRNA containing no 5′ UTR (Fig. 6*D*). Therefore, the two AUGs in the 5′ UTR of GRN repress protein translation. However, because mRNA levels of the 5′$_{AUA}$-UTR variant are still as low as with the long 5′ UTR, protein expression failed to reach the level of the GRN variant lacking the entire 5′ UTR.

Both AUGs are in the same frame, followed by an in-frame stop codon at position 159–161 (Fig. 1*B*). To further investigate the role of the uORF on repression of GRN, we investigated whether nucleotides 76–161 containing the entire uORF (Fig. 7*A*) are sufficient to suppress GRN expression. Indeed, the stretch of 50 nucleotides is sufficient to fully repress GRN expression (Fig. 7*B*). Moreover, similar findings were obtained when the same sequence was fused to the EGFP reporter (data not shown). uORFs in conjunction with appropriate secondary structures are characteristic for UTRs with translational repression properties (18–20). Therefore, these findings suggest that either ribosomes may be stalled at the upstream start codons and, consequently, be unable to efficiently initiate translation of GRN similar to the translational inhibition of BACE1 (23) or that leaky scanning or impaired reinitiation contribute to translational inhibition. Therefore, we mutagenized the two AUG codons within the uORF of the 5′ UTR to AUA ($76-161_{AUA}$) (Fig. 7*A*) and investigated the consequences on expression of GRN. Mutation of the two AUGs significantly increased expression but not to the levels of the variant lacking a 5′ UTR (Fig. 7*B*). Therefore, we investigated the potential effects on mRNA levels. Indeed, the mRNA level of the AUA ($76-161_{AUA}$) variant was reduced strongly compared with mRNA without the 5′ UTR, suggesting that reduction of mRNA prevented the full rescue of protein expression of the AUA ($76-161_{AUA}$) variant (Fig. 7*C*).

To prove that the two AUGs are involved in repression of protein translation, we performed an *in vitro* translation assay using equal amounts of *in vitro* transcribed GRN mRNA (Fig.

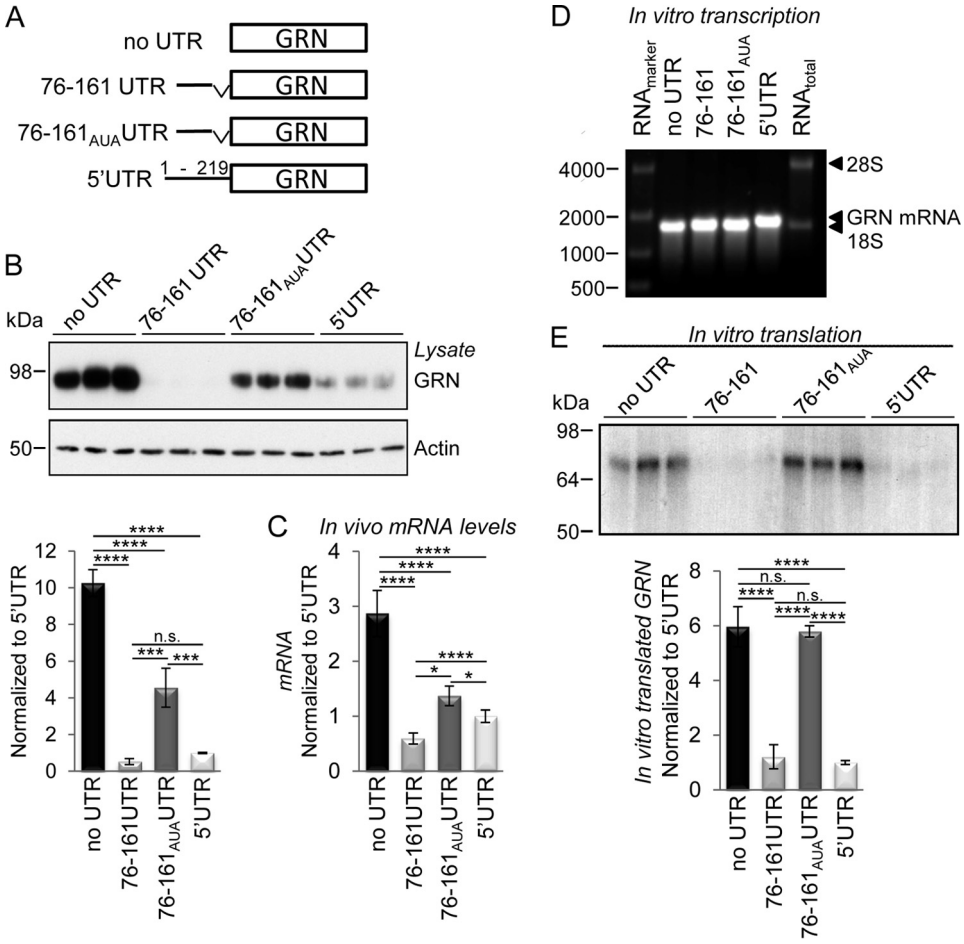

FIGURE 7. **AUGs in the uORF are responsible for translational repression of GRN but not for reducing mRNA levels.** *A*, schematic of the investigated cDNA constructs. *B*, isogenic expression of the cDNA constructs shown in *A*. Actin was used to verify equal loading. *Bottom panel*, quantitation of the expression levels of the GRN variants normalized to the 5′ UTR. Levels are normalized to expression of the 5′ UTR cDNA construct. Data are mean ± S.D. ($n \geq 3$ independent experiments). ***, $p < 0.001$; ****, $p < 0.0001$; *n.s.*, not significant. *C*, quantitation of GRN mRNA in cell lines expressing the indicated cDNA constructs normalized to the 5′ UTR construct. Data are mean ± S.D. ($n \geq 6$ independent experiments). *, $p < 0.05$; ****, $p < 0.0001$. *D*, mRNAs encoding the indicated GRN variants were transcribed *in vitro*, and equal amounts of *in vitro* transcribed mRNAs (~1 μg, adjusted to the number of nucleotides per individual mRNA) were used in *E* for in *vitro* translation. *Bottom panel*, quantitation of the expression levels of GRN upon *in vitro* translation normalized to expression of the 5′ UTR cDNA construct. Data are mean ± S.D. ($n \geq 3$ independent experiments). ****, $p < 0.0001$; *n.s.*, not significant. Significance was determined by one-way ANOVA followed by Tukey's multiple comparison test.

7*D*). Indeed, *in vitro* translation of mRNA containing nucleotides 76–161 was almost completely repressed (Fig. 7*E*). Strikingly, mutagenesis of the two AUGs was sufficient to abolish the translational inhibition (Fig. 7*E*). Therefore, the two AUGs contribute significantly to repression of GRN expression by reducing its translation.

Initiation of Translation Occurs at the Two AUGs within the uORF of GRN—To provide further evidence that the AUGs of the uORF are used for translation initiation, we generated cDNA constructs of the uORF in-frame with EGFP lacking the uORF stop codon and the EGFP start codon (76–158). This should allow monitoring of the protein production if, indeed, one of the two AUGs in the 5′ UTR is used for initiation of translation. In addition, we also individually mutated each AUG ($76–158_{AUA1}$ and $76–158_{AUA2}$) of the uORF or both in combination ($76–158_{AUA1,2}$) (Fig. 8*A*). Translation can indeed be initiated at both upstream AUGs because expression of $EGFP_{76–158}$ allowed translation of two peptides with a slightly higher molecular weight than EGFP (Fig. 8*B*). When both AUGs of the uORF are present, the first AUG is used preferentially as a start codon, as indicated by the stronger expression of the slightly higher molecular weight variant (Fig. 8*B*). Mutation of the first AUG ($76–158_{AUA1}$) abolishes the expression of the higher molecular weight variant and results in increased expression of the lower molecular weight variant, whereas mutation of the second start codon ($76–158_{AUA2}$) allows only the expression of the larger variant (Fig. 8*B*). For initiation of translation, at least one AUG of the uORF is required because the mutation of both AUGs ($76–158_{AUA1,2}$) results in a complete loss of EGFP expression. Taken together, these findings demonstrate that ribosomes can indeed use the two AUGs for initiation of translation.

An Alternatively Spliced Novel GRN Transcript That Contains a Short uORF Represses GRN Expression—Because the alternatively spliced transcript described in Fig. 1, *A* and *C*, lacks the nucleotide stretch shown above to be required for translational repression but contains an alternative uORF, we expected that this 5′ UTR variant should also be capable of repressing GRN translation. To investigate potential effects on GRN expression by this alternatively spliced 5′ UTR, we gener-

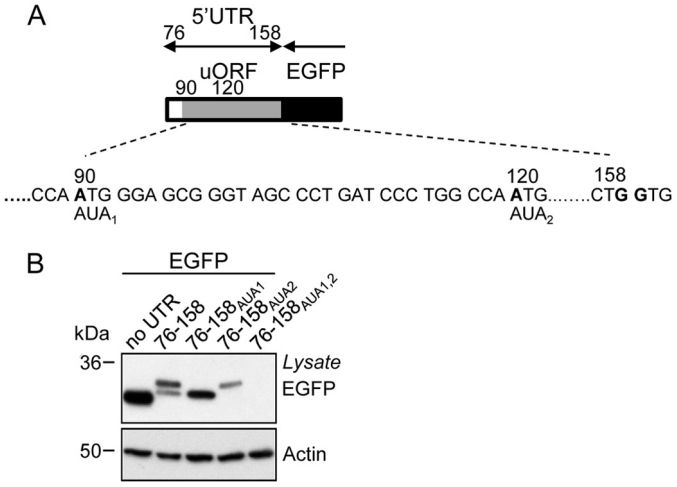

FIGURE 8. **Both AUGs in the uORF can initiate translation.** *A*, schematic of the uORF in-frame with EGFP containing a mutated start codon. The two mutated uORF start codons are indicated (AUA_1 and AUA_2). *B*, transient expression of EGFP cDNA or cDNA constructs containing nucleotides 76–158 of the 5′ UTR including both AUGs (*76–158*), either one ($76–158_{AUA1}$ and $76–158_{AUA2}$), or both ($76–158_{AUA1,2}$) mutated AUGs. Actin was used as a loading control. Note that both start codons of the uORF are functional because they are capable to initiate protein translation. The *top* and *bottom bands* represent proteins translated from the first and second AUG of the uORF. When both AUGs are mutated, no translation product can be detected.

ated a stable Flp-In™ T-REx™ HEK 293 cell line (5′$_{alt}$UTR). Expression analysis revealed that the alternative 5′ UTR suppressed GRN protein expression in a similar way as the long 5′ UTR (Fig. 9*B*). Moreover, the 5′$_{alt}$UTR also caused a reduction of mRNA levels similar to the long 5′ UTR (Fig. 9*C*). To prove that the alternative 5′ UTR also affects translational repression, we performed *in vitro* translation experiments using equal amounts of *in vitro* transcribed mRNAs (Fig. 9*D*). This revealed that the alternative 5′ UTR reduced translational efficiency as strongly as the long 5′ UTR (Fig. 9*E*). Therefore, not only the long 5′ UTR described originally but also the alternative 5′ UTR described here for the first time reduce mRNA levels and repress protein translation in parallel.

DISCUSSION

Deregulation of GRN is frequently associated with pathological conditions. Enhanced expression of GRN is observed upon lysosomal stress, inflammation, wound healing, and tumorigenesis, whereas reduced levels of GRN are associated with a significantly enhanced risk for FTLD-TDP (7). Expression of GRN is controlled on several levels. Proteolysis of GRN to granulin peptides and its inhibition by endogenous protease

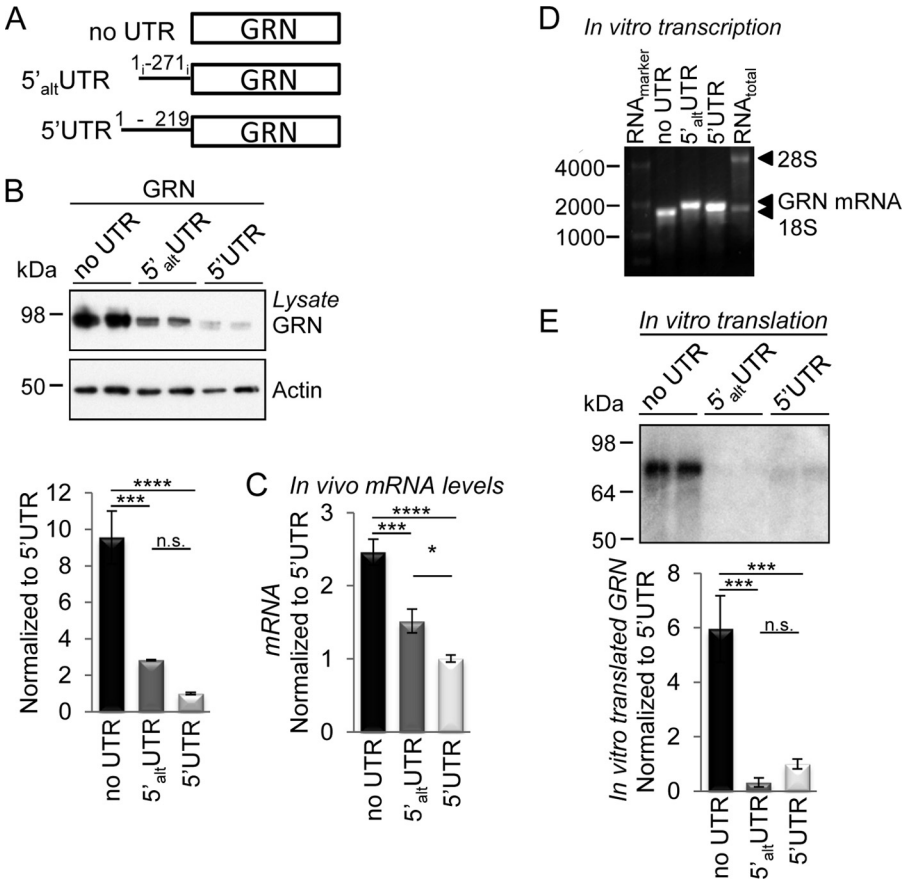

FIGURE 9. **A novel alternatively spliced variant containing two AUGs within its 5′ UTR also represses GRN expression.** *A*, schematic of the GRN 5′ UTR splice variant. *B*, isogenic expression of GRN variants in the presence and absence of the 5′ UTR or the alternative 5′$_{alt}$ UTR. Actin was used as a loading control. *Bottom panel*, quantitation of the expression levels of GRN. Data are mean ± S.D. ($n \geq 3$ independent experiments). ***, $p < 0.001$; ****$p < 0.0001$; *n.s.*, not significant. *C*, quantitation of GRN mRNA in cell lines expressing the indicated cDNA constructs normalized to the 5′ UTR construct. Data are mean ± S.D. ($n \geq 3$ independent experiments). *, $p < 0.05$; ***, $p < 0.001$; ****, $p < 0.0001$. *D*, mRNAs encoding the indicated GRN variants were transcribed *in vitro*, and equal amounts of *in vitro* transcribed mRNAs (~1 μg, adjusted to the number of nucleotides per individual mRNA) were used for *in vitro* translation. *E*, *bottom panel*, quantitation of expression levels of GRN upon *in vitro* translation of equal amounts of mRNA. For all quantifications, data are mean ± S.D. ($n = 3$ independent experiments). ***, $p < 0.001$; *n.s.*, not significant. Significance was determined by one-way ANOVA followed by Tukey's multiple comparison test. Note that the 5′$_{alt}$ UTR efficiently represses GRN expression.

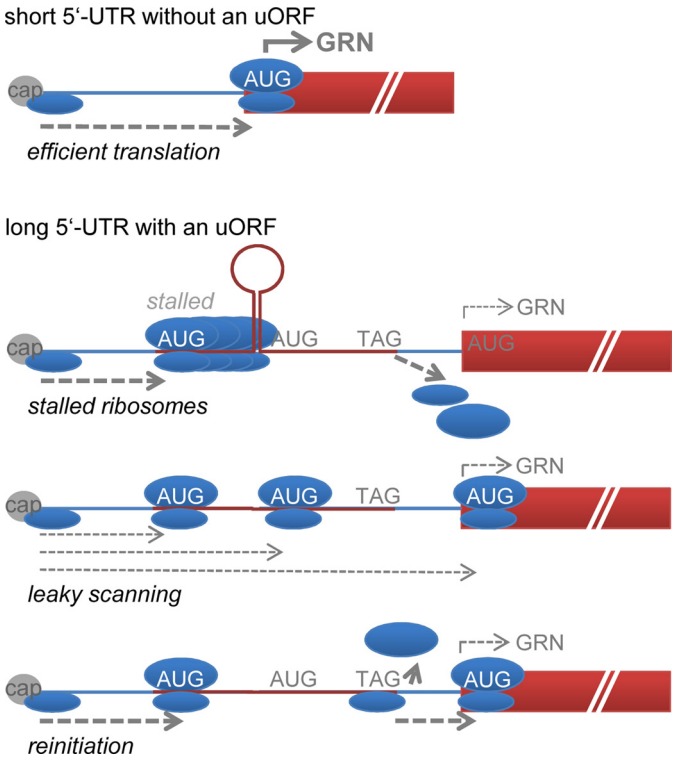

FIGURE 10. **Model explaining the dual mechanism of GRN expression control via translational inhibition and lowering of mRNA levels.** Translational inhibition may be due to stalled ribosomes, leaky scanning, and/or inefficient reinitiation at the authentic start codon of GRN.

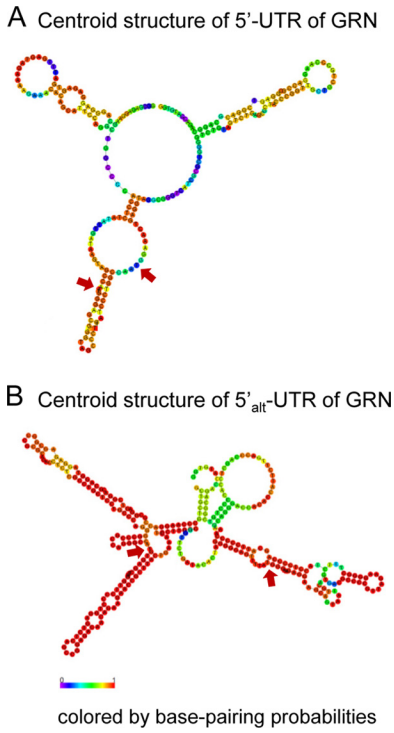

FIGURE 11. **Predicted secondary structure of the GRN 5′$_{1-219}$ UTR (*A*) and the 5′$_{alt}$ UTR (*B*).** Shown is the centroid structure encoding base pair probabilities. The bases are colored *violet* (0) for low and *red* (1) for high base-pairing probabilities. For the structure prediction, RNAfold 2.0, provided by ViennaRNA Web Services, was used. The start codons within the 5′ UTR are indicated by *arrows*.

inhibitors appears to be involved in inflammation (24). Levels of secreted GRN are regulated via receptor-mediated internalization (25). Finally, acute up-regulation of GRN levels via transcriptional (26) and posttranscriptional mechanisms (14) has been observed upon treatment with certain compounds thought to be useful in rescuing GRN haploinsufficiency in FTLD patients. However, very little is known about how GRN levels are maintained under physiological conditions. We identified a set of GRN mRNAs containing different 5′ UTRs including a so far not described alternatively spliced variant (Fig. 1). Interestingly, the 219-nucleotide 5′ UTR as well as the alternatively spliced variant harbor a potential uORF. Such 5′ UTRs with uORFs have been shown to affect the translation of several mRNAs (18–20). In line with these findings, we observed that translation of GRN is repressed selectively by the two 5′ UTR variants containing uORFs. In contrast, the shorter transcripts without an uORF occurring *in vivo*, including transcripts XM005257255 and XM005257253, are not translationally repressed (Fig. 5). In addition to a translational repression, the presence of the 5′ UTR also contributes to a reduction of mRNA levels, most likely by reducing their stability. Therefore, the 5′ UTR affects GRN expression at two levels: mRNA stability as well as translational efficacy.

We propose the following models for translational repression of GRN via its long and alternative 5′ UTR (Fig. 10). First, 40 S ribosomal subunits associated with the eIF2-GTP-Met-tRNA ternary complex scan the GRN mRNA for initiation codons, and translation will be initiated at the first AUG. Initiation at the second and third AUG (the latter being the authentic start codon for translation of GRN) may be hindered by a secondary structure located between the first two initiation codons and result in stalling of ribosomal scanning (Fig. 10, *stalled ribosomes*). Bioinformatics analysis revealed a stable loop structure between the two AUGs (Fig. 11*A*). Similarly, a very stable secondary structure is also formed by the 5′ UTR of the alternative transcript (Fig. 11*B*). Reinitiation at the third AUG codon is, therefore, a relatively unlikely event, and, consequently, translation of GRN is not very efficient, *i.e.* repressed by its 5′ UTR. In contrast, scanning of alternative transcripts lacking uORFs will result in efficient translation from the first and authentic start codon. This model is consistent with mechanisms involved in translational control of the transcription factors ATF4 or ATF5 mRNA (27). However, in line with the data in Fig. 8, our findings are also consistent with a second mechanism involving leaky scanning (Fig. 10, *leaky scanning*), whereby the 40 S ribosomal subunits associated with the eIF2-GTP-Met-tRNA ternary complex scans the 5′ UTR, and translation is initiated, to some extent, at the first and second AUG, therefore reducing translational efficacy at the third AUG. Finally, reinitiation after aborted translation of the uORF may also be considered (Fig. 10, *reinitiation*).

On the basis of our findings, one may speculate that GRN transcripts with a short 5′ UTR could cause a long term increase of GRN expression and that, under certain pathogenic conditions, initiation sites of GRN transcription or splicing may be changed and, consequently, result in dramatically different protein levels of GRN. Interestingly, Puoti *et al.* (28) just published the first FTLD-associated GRN mutation within the 5′ UTR. Strikingly, this mutation is located at the exon 1/intron 1 splice

site and results in reduction of GRN mRNA and protein levels (28).

Repression of GRN expression is likely to be supported by RNA binding proteins. Such proteins may be degraded under stress conditions and, therefore, indirectly facilitate translation as a fast response, for example, to injury. In addition, in that regard, it is also interesting to note that many proteins that are genetically associated with ALS or FTLD, such as TDP-43 (29), Fused in sarcoma (30, 31), heterogeneous ribonucleoprotein (hnRNP) A1, and hnRNP A2B1 (32), are well known RNA-binding proteins involved in translation, mRNA transport, and RNA splicing. If any of these proteins are involved in translational repression of GRN remains to be shown. However, it is tempting to speculate that pharmaceutical interference with such binding proteins could be used to therapeutically modulate GRN expression under various pathological conditions.

Acknowledgments—We thank Drs. Sven Lammich, Michael Willem, and Gernot Kleinberger for critical reading of the manuscript and Dr. Kohji Mori for helpful suggestions.

REFERENCES

1. Graff-Radford, N. R., and Woodruff, B. K. (2007) Frontotemporal dementia. *Semin. Neurol.* **27,** 48–57
2. Ratnavalli, E., Brayne, C., Dawson, K., and Hodges, J. R. (2002) The prevalence of frontotemporal dementia. *Neurology* **58,** 1615–1621
3. Rademakers, R., Neumann, M., and Mackenzie, I. R. (2012) Advances in understanding the molecular basis of frontotemporal dementia. *Nat. Rev. Neurol.* **8,** 423–434
4. Neumann, M., Sampathu, D. M., Kwong, L. K., Truax, A. C., Micsenyi, M. C., Chou, T. T., Bruce, J., Schuck, T., Grossman, M., Clark, C. M., McCluskey, L. F., Miller, B. L., Masliah, E., Mackenzie, I. R., Feldman, H., Feiden, W., Kretzschmar, H. A., Trojanowski, J. Q., and Lee, V. M. (2006) Ubiquitinated TDP-43 in frontotemporal lobar degeneration and amyotrophic lateral sclerosis. *Science* **314,** 130–133
5. Baker, M., Mackenzie, I. R., Pickering-Brown, S. M., Gass, J., Rademakers, R., Lindholm, C., Snowden, J., Adamson, J., Sadovnick, A. D., Rollinson, S., Cannon, A., Dwosh, E., Neary, D., Melquist, S., Richardson, A., Dickson, D., Berger, Z., Eriksen, J., Robinson, T., Zehr, C., Dickey, C. A., Crook, R., McGowan, E., Mann, D., Boeve, B., Feldman, H., and Hutton, M. (2006) Mutations in progranulin cause Tau-negative frontotemporal dementia linked to chromosome 17. *Nature* **442,** 916–919
6. Cruts, M., Gijselinck, I., van der Zee, J., Engelborghs, S., Wils, H., Pirici, D., Rademakers, R., Vandenberghe, R., Dermaut, B., Martin, J. J., van Duijn, C., Peeters, K., Sciot, R., Santens, P., De Pooter, T., Mattheijssens, M., Van den Broeck, M., Cuijt, I., Vennekens, K., De Deyn, P. P., Kumar-Singh, S., and Van Broeckhoven, C. (2006) Null mutations in progranulin cause ubiquitin-positive frontotemporal dementia linked to chromosome 17q21. *Nature* **442,** 920–924
7. Kleinberger, G., Capell, A., Haass, C., and Van Broeckhoven, C. (2013) Mechanisms of granulin deficiency: lessons from cellular and animal models. *Mol. Neurobiol.* **47,** 337–360
8. Schymick, J. C., Yang, Y., Andersen, P. M., Vonsattel, J. P., Greenway, M., Momeni, P., Elder, J., Chiò, A., Restagno, G., Robberecht, W., Dahlberg, C., Mukherjee, O., Goate, A., Graff-Radford, N., Caselli, R. J., Hutton, M., Gass, J., Cannon, A., Rademakers, R., Singleton, A. B., Hardiman, O., Rothstein, J., Hardy, J., and Traynor, B. J. (2007) Progranulin mutations and amyotrophic lateral sclerosis or amyotrophic lateral sclerosis-frontotemporal dementia phenotypes. *J. Neurol. Neurosurg. Psychiatry* **78,** 754–756
9. van der Zee, J., Le Ber, I., Maurer-Stroh, S., Engelborghs, S., Gijselinck, I., Camuzat, A., Brouwers, N., Vandenberghe, R., Sleegers, K., Hannequin, D., Dermaut, B., Schymkowitz, J., Campion, D., Santens, P., Martin, J. J., Lacomblez, L., De Pooter, T., Peeters, K., Mattheijssens, M., Vercelletto, M., Van den Broeck, M., Cruts, M., De Deyn, P. P., Rousseau, F., Brice, A., and Van Broeckhoven, C. (2007) Mutations other than null mutations producing a pathogenic loss of progranulin in frontotemporal dementia. *Hum. Mutat.* **28,** 416
10. Brouwers, N., Sleegers, K., Engelborghs, S., Maurer-Stroh, S., Gijselinck, I., van der Zee, J., Pickut, B. A., Van den Broeck, M., Mattheijssens, M., Peeters, K., Schymkowitz, J., Rousseau, F., Martin, J. J., Cruts, M., De Deyn, P. P., and Van Broeckhoven, C. (2008) Genetic variability in progranulin contributes to risk for clinically diagnosed Alzheimer disease. *Neurology* **71,** 656–664
11. Shankaran, S. S., Capell, A., Hruscha, A. T., Fellerer, K., Neumann, M., Schmid, B., and Haass, C. (2008) Missense mutations in the progranulin gene linked to frontotemporal lobar degeneration with ubiquitin-immunoreactive inclusions reduce progranulin production and secretion. *J. Biol. Chem.* **283,** 1744–1753
12. Mukherjee, O., Wang, J., Gitcho, M., Chakraverty, S., Taylor-Reinwald, L., Shears, S., Kauwe, J. S., Norton, J., Levitch, D., Bigio, E. H., Hatanpaa, K. J., White, C. L., Morris, J. C., Cairns, N. J., and Goate, A. (2008) Molecular characterization of novel progranulin (GRN) mutations in frontotemporal dementia. *Hum. Mutat.* **29,** 512–521
13. Smith, K. R., Damiano, J., Franceschetti, S., Carpenter, S., Canafoglia, L., Morbin, M., Rossi, G., Pareyson, D., Mole, S. E., Staropoli, J. F., Sims, K. B., Lewis, J., Lin, W. L., Dickson, D. W., Dahl, H. H., Bahlo, M., and Berkovic, S. F. (2012) Strikingly different clinicopathological phenotypes determined by progranulin-mutation dosage. *Am. J. Hum. Genet.* **90,** 1102–1107
14. Capell, A., Liebscher, S., Fellerer, K., Brouwers, N., Willem, M., Lammich, S., Gijselinck, I., Bittner, T., Carlson, A. M., Sasse, F., Kunze, B., Steinmetz, H., Jansen, R., Dormann, D., Sleegers, K., Cruts, M., Herms, J., Van Broeckhoven, C., and Haass, C. (2011) Rescue of progranulin deficiency associated with frontotemporal lobar degeneration by alkalizing reagents and inhibition of vacuolar ATPase. *J. Neurosci.* **31,** 1885–1894
15. Lammich, S., Schöbel, S., Zimmer, A. K., Lichtenthaler, S. F., and Haass, C. (2004) Expression of the Alzheimer protease BACE1 is suppressed via its 5′-untranslated region. *EMBO Rep.* **5,** 620–625
16. Lammich, S., Buell, D., Zilow, S., Ludwig, A. K., Nuscher, B., Lichtenthaler, S. F., Prinzen, C., Fahrenholz, F., and Haass, C. (2010) Expression of the anti-amyloidogenic secretase ADAM10 is suppressed by its 5′-untranslated region. *J. Biol. Chem.* **285,** 15753–15760
17. Kozak, M. (1986) Point mutations define a sequence flanking the AUG initiator codon that modulates translation by eukaryotic ribosomes. *Cell* **44,** 283–292
18. Liu, L., Dilworth, D., Gao, L., Monzon, J., Summers, A., Lassam, N., and Hogg, D. (1999) Mutation of the CDKN2A 5′ UTR creates an aberrant initiation codon and predisposes to melanoma. *Nat. Genet.* **21,** 128–132
19. Wiestner, A., Schlemper, R. J., van der Maas, A. P., and Skoda, R. C. (1998) An activating splice donor mutation in the thrombopoietin gene causes hereditary thrombocythaemia. *Nat. Genet.* **18,** 49–52
20. Wen, Y., Liu, Y., Xu, Y., Zhao, Y., Hua, R., Wang, K., Sun, M., Li, Y., Yang, S., Zhang, X. J., Kruse, R., Cichon, S., Betz, R. C., Nöthen, M. M., van Steensel, M. A., van Geel, M., Steijlen, P. M., Hohl, D., Huber, M., Dunnill, G. S., Kennedy, C., Messenger, A., Munro, C. S., Terrinoni, A., Hovnanian, A., Bodemer, C., de Prost, Y., Paller, A. S., Irvine, A. D., Sinclair, R., Green, J., Shang, D., Liu, Q., Luo, Y., Jiang, L., Chen, H. D., Lo, W. H., McLean, W. H., He, C. D., and Zhang, X. (2009) Loss-of-function mutations of an inhibitory upstream ORF in the human hairless transcript cause Marie Unna hereditary hypotrichosis. *Nat. Genet.* **41,** 228–233
21. Calvo, S. E., Pagliarini, D. J., and Mootha, V. K. (2009) Upstream open reading frames cause widespread reduction of protein expression and are polymorphic among humans. *Proc. Natl. Acad. Sci. U.S.A.* **106,** 7507–7512
22. Barbosa, C., Peixeiro, I., and Romão, L. (2013) Gene expression regulation by upstream open reading frames and human disease. *PLoS Genet.* **9,** e1003529
23. O'Connor, T., Sadleir, K. R., Maus, E., Velliquette, R. A., Zhao, J., Cole, S. L., Eimer, W. A., Hitt, B., Bembinster, L. A., Lammich, S., Lichtenthaler, S. F., Hébert, S. S., De Strooper, B., Haass, C., Bennett, D. A., and Vassar, R. (2008) Phosphorylation of the translation initiation factor eIF2α increases BACE1 levels and promotes amyloidogenesis. *Neuron* **60,** 988–1009

24. Bateman, A., and Bennett, H. P. (2009) The granulin gene family: from cancer to dementia. *BioEssays* **31,** 1245–1254
25. Hu, F., Padukkavidana, T., Vægter, C. B., Brady, O. A., Zheng, Y., Mackenzie, I. R., Feldman, H. H., Nykjaer, A., and Strittmatter, S. M. (2010) Sortilin-mediated endocytosis determines levels of the frontotemporal dementia protein, progranulin. *Neuron* **68,** 654–667
26. Cenik, B., Sephton, C. F., Dewey, C. M., Xian, X., Wei, S., Yu, K., Niu, W., Coppola, G., Coughlin, S. E., Lee, S. E., Dries, D. R., Almeida, S., Geschwind, D. H., Gao, F. B., Miller, B. L., Farese, R. V., Jr., Posner, B. A., Yu, G., and Herz, J. (2011) Suberoylanilide hydroxamic acid (vorinostat) upregulates progranulin transcription: rational therapeutic approach to frontotemporal dementia. *J. Biol. Chem.* **286,** 16101–16108
27. Jackson, R. J., Hellen, C. U., and Pestova, T. V. (2010) The mechanism of eukaryotic translation initiation and principles of its regulation. *Nat. Rev. Mol. Cell Biol.* **11,** 113–127
28. Puoti, G., Lerza, M. C., Ferretti, M. G., Bugiani, O., Tagliavani, F., Rossi, G. (2014) A mutation of the 5′-UTR of GRN gene associated with frontotemporal lobar degeneration: phenotypic variability and possible pathogenic mechanisms. *J. Alzheimer's Dis.*, in press
29. Sreedharan, J., Blair, I. P., Tripathi, V. B., Hu, X., Vance, C., Rogelj, B., Ackerley, S., Durnall, J. C., Williams, K. L., Buratti, E., Baralle, F., de Belleroche, J., Mitchell, J. D., Leigh, P. N., Al-Chalabi, A., Miller, C. C., Nicholson, G., and Shaw, C. E. (2008) TDP-43 mutations in familial and sporadic amyotrophic lateral sclerosis. *Science* **319,** 1668–1672
30. Kwiatkowski, T. J., Jr., Bosco, D. A., Leclerc, A. L., Tamrazian, E., Vanderburg, C. R., Russ, C., Davis, A., Gilchrist, J., Kasarskis, E. J., Munsat, T., Valdmanis, P., Rouleau, G. A., Hosler, B. A., Cortelli, P., de Jong, P. J., Yoshinaga, Y., Haines, J. L., Pericak-Vance, M. A., Yan, J., Ticozzi, N., Siddique, T., McKenna-Yasek, D., Sapp, P. C., Horvitz, H. R., Landers, J. E., and Brown, R. H., Jr. (2009) Mutations in the FUS/TLS gene on chromosome 16 cause familial amyotrophic lateral sclerosis. *Science* **323,** 1205–1208
31. Vance, C., Rogelj, B., Hortobágyi, T., De Vos, K. J., Nishimura, A. L., Sreedharan, J., Hu, X., Smith, B., Ruddy, D., Wright, P., Ganesalingam, J., Williams, K. L., Tripathi, V., Al-Saraj, S., Al-Chalabi, A., Leigh, P. N., Blair, I. P., Nicholson, G., de Belleroche, J., Gallo, J. M., Miller, C. C., and Shaw, C. E. (2009) Mutations in FUS, an RNA processing protein, cause familial amyotrophic lateral sclerosis type 6. *Science* **323,** 1208–1211
32. Kim, H. J., Kim, N. C., Wang, Y. D., Scarborough, E. A., Moore, J., Diaz, Z., MacLea, K. S., Freibaum, B., Li, S., Molliex, A., Kanagaraj, A. P., Carter, R., Boylan, K. B., Wojtas, A. M., Rademakers, R., Pinkus, J. L., Greenberg, S. A., Trojanowski, J. Q., Traynor, B. J., Smith, B. N., Topp, S., Gkazi, A. S., Miller, J., Shaw, C. E., Kottlors, M., Kirschner, J., Pestronk, A., Li, Y. R., Ford, A. F., Gitler, A. D., Benatar, M., King, O. D., Kimonis, V. E., Ross, E. D., Weihl, C. C., Shorter, J., and Taylor, J. P. (2013) Mutations in prion-like domains in hnRNPA2B1 and hnRNPA1 cause multisystem proteinopathy and ALS. *Nature* **495,** 467–473